

Origin of similarity of phase diagrams in amphiphilic and colloidal systems with competing interactions

A. Ciach, J. Pękalski and W. T. Gózdź

Institute of Physical Chemistry, Polish Academy of Sciences, 01-224 Warszawa, Poland

(Dated: August 8, 2018)

Abstract

We show that amphiphilic and colloidal systems with competing interactions can be described by the same Landau-Brazovskii functional. The functional is obtained by a systematic coarse-graining procedure applied to systems with isotropic interaction potentials. Microscopic expressions for the coefficients in the functional are derived. We propose simple criteria to distinguish the effective interparticle potentials that can lead to macro- or microsegregation. Our considerations concern also charged globular proteins in aqueous solutions and other system with effective short-range attraction long-range repulsion interactions.

I. INTRODUCTION

Recent experimental [1–4], simulation [5–7] and theoretical studies [8–13] have revealed striking similarity between colloidal and amphiphilic self-assembly, despite different interaction potentials in such systems. Interactions between amphiphilic molecules are strongly orientation-dependent, whereas effective interactions between spherical colloid particles usually depend only on the distance between their centers. When particles are charged and polymers are present in solution, short-range depletion attraction competes with long-range electrostatic repulsion [1–3, 14] (SALR potential). The SALR potential is important for many other soft-matter and biological systems, because both the colloid particles and the macromolecules in water are typically charged and repel each other with screened electrostatic forces, and in addition attract each other with van der Waals and solvent-induced solvophobic[15–17] or thermodynamic Casimir forces [18–21]. Attraction leads to cluster formation, but further growth of the clusters is suppressed by sufficiently strong repulsion [22] when the size of the cluster becomes comparable with the range of the repulsion. For increasing concentration of colloidal particles spherical clusters (droplets), elongated clusters, slabs, cylindrical voids (bubbles) and spherical voids were seen in MC simulation[7]. When the clusters, rods, slabs or voids are periodically distributed in space, ordered soft crystals are formed. The hexagonal and lamellar phases and transitions between them were discovered in MD [5] and MC [6] simulations. Transitions between the lamellar phase and the hexagonal phases of droplets and bubbles were also predicted by density functional theory (DFT) [10]. For intermediate densities a network of particles was obtained by Brownian dynamics simulations [23, 24]. Similar phase diagrams but with micelles, reverse micelles, bilayers and bicontinuous phases instead of, respectively, clusters (droplets), voids (bubbles), slabs and networks of particles were obtained for water-surfactant mixtures and for block copolymers[25–28] (see Fig.1).

Experimental studies confirmed existence of spherical and elongated clusters, as well as particle networks [1–4]. The ordered phases have not been discovered yet, because many long-lived metastable states are present, and in confocal microscopy observations [2, 3] instantaneous, rather than average distributions of particles were observed. Average distribution can be obtained from dynamical confocal microscopy measurements, and in the future such experiments should be conducted in order to obtain phase diagrams. Reliable determi-

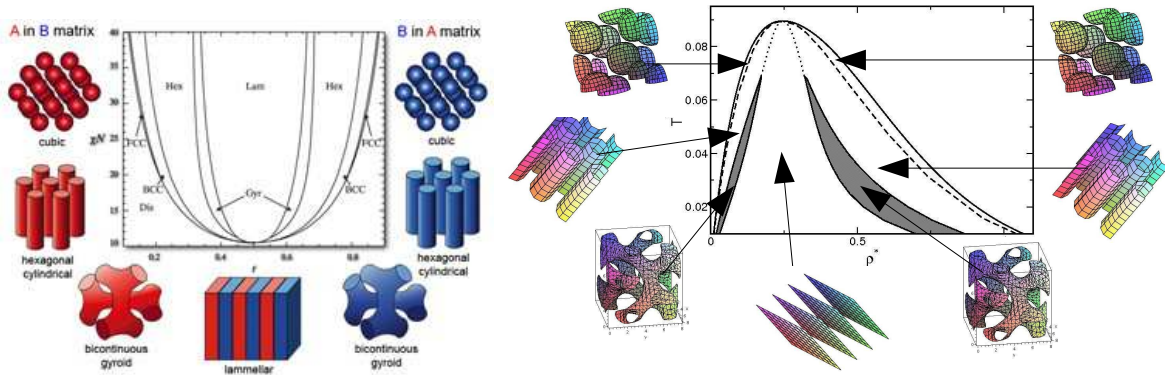


FIG. 1: Top panel: phase diagram in block copolymer system (reprinted from Ref.[27]). f is the ratio between the number of the A and B monomers and the Flory parameter χ is inversely proportional to temperature T . Bottom panel: phase diagram in the SALR-potential system obtained in Refs.[11, 12]. $\rho^* = 6\eta/\pi$, where η is the volume fraction of particles. The structure of the phases stable in regions separated by the solid, dashed and dotted lines is illustrated by the corresponding surfaces placed around the phase diagram. Inside the regions enclosed by these surfaces the density is enhanced or depleted compared to ρ^* when $\rho^* < 0.25$ or $\rho^* > 0.25$ respectively.

nation of phase diagrams in simulations is also nontrivial because of the long-lived metastable states [23], and suitable simulation procedures (e.g. the one suggested in Ref. [29]) are required. Because of these difficulties, theoretical predictions are necessary to guide both experiment and simulations.

The purpose of this work is to understand origin of the similarity between the phase diagrams in amphiphilic systems and in systems interacting with the SALR type potentials. Once the mapping between the mathematical models describing these systems is established, one can take advantage of the results obtained earlier for the amphiphilic systems in studies of systems with competing interactions.

It is well known that the topology of the phase diagrams in systems undergoing separation into homogeneous phases is the same [30]. This universality is reflected in the generic Landau functional [30] of the order parameter (OP) ϕ (e.g. a deviation of the density from its critical value),

$$\mathcal{L} = \int d\mathbf{r} \left[f(\phi(\mathbf{r})) + \frac{\beta V_2}{2} |\nabla \phi(\mathbf{r})|^2 \right], \quad (1)$$

where $f(\phi) = (A_2/2 + \beta V_0)\phi^2 + A_4\phi^4/4!$, $\beta = (k_B T)^{-1}$, k_B is the Boltzmann constant and T is the temperature, $V_0 < 0$ is the measure of attraction, $A_n > 0$ and $V_2 > 0$. The term $\beta V_2 |\nabla\phi(\mathbf{r})|^2/2$ ensures that the phases corresponding to the minimum of the functional (1) are homogeneous ($\nabla\phi(\mathbf{r}) = 0$).

In order to describe microsegregation in systems with competing interactions, several authors extended the functional (1) by including different repulsive terms [8, 9, 31]. Unfortunately, such an approach suffers from an inconsistent treatment of the attractive and repulsive parts of interactions; while the former is included in the coarse-grained functional, the latter has a microscopic form. Universal emergence of modulated phases was noted in these and other studies, but it remains unclear why the pattern formation in the presence of frustration should be the same as in amphiphilic systems. In contrast to simple systems that are all described by the same functional (1), universal ordering on the mesoscopic length scale was not related to a generic functional common for all microsegregating systems.

The functional successfully used for block copolymers and microemulsions has the form [25, 26, 28, 32, 33]

$$\mathcal{L}_B = \int d\mathbf{r} \left[f(\phi(\mathbf{r})) + \frac{\beta V_2}{2} |\nabla\phi(\mathbf{r})|^2 + \frac{\beta V_4}{4!} (\nabla^2\phi(\mathbf{r}))^2 \right] \quad (2)$$

with $V_2 < 0$ and $V_4 > 0$. The inhomogeneous structure is favored and disfavored by the second and the third term in (2) respectively. Competition between these terms leads to a finite length scale of inhomogeneities, $2\pi/k_b$, with $k_b^2 = -6V_2/V_4$ [34]. We should mention that the functional (2) has essentially the same form as the free energy functional in the phase-field-crystal (PFC) model of freezing and pattern formation on atomistic length scale [35].

Because the functional (2) describes successfully various inhomogeneous systems, it is plausible that the generic model for systems with competing interactions has the same form, with $\phi(\mathbf{r})$ denoting local excess volume fraction of particles. However, it is not obvious a priori if the functional (1) with $V_2 > 0$ or (2) with $V_2 < 0$ is appropriate for a given form of interactions. Thus, it is necessary to find the relation between the coefficients in the functional and the form of the interaction potential. Such a relation can be reliably obtained when the functional (2) is derived from a microscopic theory.

In this work we consider effectively one-component systems of particles interacting with spherically symmetric potentials of arbitrary form. Solvent molecules and depletion agents

are taken into account indirectly in the form of effective interactions between the particles. In sec.2 we derive approximate expression for the internal energy. In sec.3 we derive and discuss the Landau-Brazovskii functional. The effective potentials are classified in sec.4. Sec.5 contains short summary and discussion.

II. APPROXIMATE EXPRESSIONS FOR THE INTERNAL ENERGY

Let us focus on the internal energy (configurational part),

$$\mathcal{U} = \frac{1}{2} \int d\mathbf{r} \int d\Delta\mathbf{r} \rho(\mathbf{r})\rho(\mathbf{r} + \Delta\mathbf{r})V(\Delta r)g(\Delta r) \quad (3)$$

where $V(\Delta r)$ and $g(\Delta r)$ are the interaction potential and the pair distribution function for particles located at \mathbf{r} and $\mathbf{r} + \Delta\mathbf{r}$, and $\rho(\mathbf{r})$ is the local average density of the particles. We focus on systems inhomogeneous on a mesoscopic length scale and on weak ordering, therefore we assume that g depends only on Δr , and $\rho(\mathbf{r})$ is a slowly varying function.

A. Short-range interaction potentials

In the first step we consider short-range interaction potentials, whose moments $\int d\mathbf{r}V(r)r^n$ are finite at least for $n = 4$. We Taylor expand $\rho(\mathbf{r} + \Delta\mathbf{r})$ about \mathbf{r} , integrate by parts (see Appendix) and obtain the following approximate expression for the internal energy (3)

$$\mathcal{U} \approx \int d\mathbf{r} [V_0\eta(\mathbf{r})^2 + \frac{V_2}{2}|\nabla\eta(\mathbf{r})|^2 + \dots] \quad (4)$$

where $\eta(\mathbf{r}) = \rho(\mathbf{r})v$ is the local volume fraction, $v = \pi\sigma^3/6$ is the particle volume, and

$$V_n = \frac{2\pi(-1)^{n/2}}{(n+1)v^2} \int_0^\infty dr r^{2+n}V(r)g(r). \quad (5)$$

For attractive interactions ($Vg < 0$) homogeneous phases are energetically favored, because $V_2 > 0$, and the second term in (4) leads to an *increase* of \mathcal{U} for $\nabla\eta(\mathbf{r}) \neq 0$. Note that $g > 0$ and either oscillates around 1 in crystals or exhibits oscillatory decay to 1 in liquids. Thus, repulsion at large distances ($Vg > 0$) can lead to $V_2 < 0$, and hence to a *decrease* of \mathcal{U} for $\nabla\eta(\mathbf{r}) \neq 0$, i.e. to spatial inhomogeneities. For an illustration we plot $V(r)r^n$ in Fig.2 for the double Yukawa potential [7, 36]

$$V(r) = -K_1 \frac{\exp(-z_1 r)}{r} + K_2 \frac{\exp(-z_2 r)}{r}. \quad (6)$$

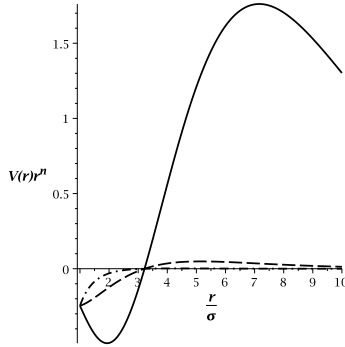


FIG. 2: $V(r)r^n$ for $n = 4$ (solid line), $n = 2$ (dash line) and $n = 0$ (dash-dot line), for the SALR potential (6) with $K_1 = 1, K_2 = 0.2, z_1 = 1, z_2 = 0.5$. Note that the large positive integrand can lead to a positive integral $\int_0^\infty dr r^4 V(r)$. Because $g > 0$ and for large distances approaches 1 (or oscillates around 1 in the case of crystalline order inside the clusters), we obtain $V_2 < 0$ (see (5)). Note also that the above argument is not restricted to the potential (6), but holds for any spherically-symmetric interaction potential assuming large positive value for large r .

For $V_2 < 0$ the Taylor expansion of $\rho(\mathbf{r} + \Delta\mathbf{r})$ should be truncated at the fourth order term, and (4) should be replaced by (see Appendix)

$$\mathcal{U} \approx \int d\mathbf{r} \left[V_0 \eta(\mathbf{r})^2 + \frac{V_2}{2} |\nabla \eta(\mathbf{r})|^2 + \frac{V_4}{4!} (\nabla^2 \eta(\mathbf{r}))^2 \right]. \quad (7)$$

From (5) it follows that $V_4 > 0$ if $V_2 < 0$, and the above functional is stable. Note the similarity between the last two terms in Eqs.(7) and (2). Spatial inhomogeneities favored by Eq.(7) for $V_2 < 0$ are consistent with preferential formation of clusters in the case of the SALR potential, with the size and the distance between the clusters determined by the range of attraction and the range of repulsion respectively.

B. Long-range interaction potentials

The above considerations are valid for potentials that decay faster than $1/r^7$ (see (5)). For the long-range potentials whose moments (5) diverge, the expansion (7) of the internal energy (3) is not valid. However, the internal energy can be approximated by Eq.(7) even for long-range interactions, but with V_n given in terms of the Fourier transform

$$\tilde{V}_g(k) = \int d\mathbf{r} \exp(i\mathbf{k} \cdot \mathbf{r}) \frac{V(r)g(r)}{v^2}, \quad (8)$$

which for $k > 0$ may exist even when the moments in (5) diverge. Eqs.(3) and (7) in Fourier representation take the forms

$$\mathcal{U} = \frac{1}{2} \int \frac{d\mathbf{k}}{(2\pi)^3} \tilde{V}_g(k) |\tilde{\eta}(\mathbf{k})|^2, \quad (9)$$

and

$$\mathcal{U} \approx \int \frac{d\mathbf{k}}{(2\pi)^3} \left(V_0 + \frac{V_2}{2} k^2 + \frac{V_4}{4!} k^4 \right) |\tilde{\eta}(\mathbf{k})|^2, \quad (10)$$

where $\tilde{\eta}(\mathbf{k}) = \int d\mathbf{r} \exp(i\mathbf{k} \cdot \mathbf{r}) \eta(\mathbf{r})$. Note that Eq.(10) is obtained when $\tilde{V}_g(k)$ in Eq.(9) is approximated by a truncated Taylor expansion in small k . When V_n defined in Eq.(5) diverge, $\tilde{V}_g(k)$ is nonanalytic at $k = 0$ and Eq.(10) is not valid.

In order to develop appropriate approximate expression for U in such a case, let us consider a change of the internal energy (3) per unit volume associated with formation of the mesoscopic inhomogeneity $\eta_0 \rightarrow \eta(\mathbf{r}) = \eta_0 + \phi(\mathbf{r})$. For the planar density-wave $\phi(\mathbf{r}) = \phi_k \cos(kz)$ we have

$$\Delta u = \phi_k^2 \tilde{V}_g(k) / 4. \quad (11)$$

When the amplitude of the density modulations ϕ_k is fixed, Δu takes the minimum at $k = k_b$, corresponding to the minimum of $\tilde{V}_g(k)$. Thus, the energetically favored length scale of inhomogeneity is $2\pi/k_b$. Spatial inhomogeneities can lead to a decrease of the internal energy if

$$\tilde{V}_g(k_b) < 0. \quad (12)$$

If $k_b > 0$ and is not very small, then $\tilde{V}_g(k)$ should be expanded about its minimum at $k = k_b$, rather than about $k = 0$ where it may be nonanalytic. When the minimum of $\tilde{V}_g(k)$ at $k = k_b$ is deep, the waves with $k \approx k_b$ lead to much lower Δu (see (11)) than the waves with k significantly different from k_b . For this reason the waves with $k \approx k_b$ are thermally excited with much higher probability than the waves with k significantly different from k_b . For the potentials with deep minimum at $k = k_b \neq 0$ the expansion of $\tilde{V}_g(k)$ about $k = k_b$ can be truncated, because for small values of $|k - k_b|$ the truncated Taylor expansion is close to $\tilde{V}_g(k)$. On the other hand, the waves with the wavenumbers k much different from k_b are excited with negligible probability and can be disregarded. If we require that the approximate expression for \tilde{V}_g is an even function of k , then for $k_b > 0$ we obtain

$$\tilde{V}_g(k) \approx \tilde{V}_g(k_b) + v_2(k^2 - k_b^2)^2 / 2 \quad (13)$$

where $v_2 = \tilde{V}_g''(k_b)/(2k_b)^2$. When (13) is inserted in (9) and the relations between $k^n \tilde{\eta}(\mathbf{k})$ and $\nabla^n \eta(\mathbf{r})$ are taken into account, then Eq.(9) in real space representation takes the form (7) but with V_n given by

$$V_0 = \frac{1}{2}(\tilde{V}_g(k_b) + v_2 k_b^4/2), V_2 = -v_2 k_b^2, V_4 = 6v_2. \quad (14)$$

The above holds only for $k_b > 0$. We finally stress that Eq.(7) can be used provided that (13) is a reasonable approximation for $\tilde{V}_g(k)$; if it is not, the internal energy given in Eq.(9) cannot be simplified according to the above scheme and the functional (7) is not valid. We further discuss this issue in sec.4.

III. DERIVATION OF THE LANDAU-BRAZOVSKII FUNCTIONAL

In order to find thermal equilibrium we need to compare grand potentials in systems with and without mesoscopic inhomogeneities. A particular form of the volume fraction on the mesoscopic scale, $\eta(\mathbf{r})$, imposes a constraint on the volume occupied by the particles in mesoscopic regions [11]. Let us consider the grand potential in the presence of the constraint $\eta(\mathbf{r})$,

$$\Omega_{co}[\eta] = U[\eta] - TS[\eta] - \bar{\mu} \int d\mathbf{r} \eta(\mathbf{r}), \quad (15)$$

where $U[\eta]$ and $S[\eta]$ are the configurational parts of the internal energy and the entropy, $\bar{\mu} = [\mu - k_B T \ln(\Lambda/\sigma)^3]/v$ and Λ is the thermal wavelength. We assume that $U[\eta]$ is given by (4) or (7), except that g in (5) and (8) should be replaced by g_{co} calculated for the fixed mesoscopic state $\eta(\mathbf{r})$.

When $\eta(\mathbf{r})$ varies on a length scale larger than σ , then we can make the local density approximation for the entropy, $-TS \approx \int d\mathbf{r} [f_h(\eta(\mathbf{r}))]$, where $f_h(\eta)$ is the configurational part of the free energy density of the hard-sphere reference system with the volume fraction η . $f_h(\eta_0 + \phi(\mathbf{r}))$ can be Taylor expanded. Note that by definition the local volume fraction $\eta(\mathbf{r}) = v\rho(\mathbf{r}) < 1$. Local deviations $\phi(\mathbf{r}) = \eta(\mathbf{r}) - \eta_0$ from the space-average volume fraction η_0 are $|\phi(\mathbf{r})| < 1$, and the truncation of the Taylor series for $f_h(\eta_0 + \phi(\mathbf{r}))$ is justified. For weak ordering ($\phi(\mathbf{r}) \ll 1$) $f_h(\eta)$ can be approximated by the polynomial in ϕ .

From (15), (4), (7) and the above we can see that the change of $\beta\Omega_{co}$ associated with creation of the mesoscopic inhomogeneity,

$$\mathcal{L}_{\eta_0}[\phi] = \beta\Omega_{co}[\eta_0 + \phi] - \beta\Omega_{co}[\eta_0], \quad (16)$$

takes the form of the functional (1) or (2) for $V_2 > 0$ or $V_2 < 0$ respectively, with

$$f(\phi) = \sum_{n \geq 1} \frac{1}{n!} \left. \frac{d^n \beta f_h(\eta)}{d\eta^n} \right|_{\eta=\eta_0} \phi^n + 2\eta_0 \beta V_0 \phi + \beta V_0 \phi^2 - \beta \bar{\mu} \phi. \quad (17)$$

Thus, we have shown that self-assembly in amphiphilic systems and in systems with competing interactions can be described by the same functional (2). This explains striking similarity of the phase diagrams.

The phase diagrams in Fig.1 and earlier results [25, 26] obtained by minimization of the functional (2) are in good qualitative agreement with the DFT results [10], and both theories are in qualitative agreement with simulations. In simulations the modulated phases are stable in a smaller region of the phase diagram (the disordered phase becomes stable at lower T than found in MF), and the transition between the disordered and lamellar phases occurs for a much larger temperature interval [5, 6]. To explain these discrepancies, let us note that $\Omega_{co}[\eta]$ is calculated for the specified mesoscopic volume fraction $\eta(\mathbf{r})$. A probability of spontaneous appearance of $\eta(\mathbf{r})$ is $p[\eta] \propto \exp(-\beta \Omega_{co}[\eta])$ [11, 30]. The inhomogeneous and homogeneous states occur with the same probability when $\mathcal{L}_{\eta_0}[\phi] = 0$, since $p[\eta_0 + \phi]/p[\eta_0] = \exp(-\mathcal{L}_{\eta_0}[\phi])$. This should not be mistaken with thermodynamic equilibrium associated with equality of the grand potentials

$$\beta \Omega[\bar{\eta}] = \beta \Omega_{co}[\bar{\eta}] - \ln \left[\int D\psi e^{-\beta H_{fluc}[\bar{\eta}, \psi]} \right] \quad (18)$$

where $\bar{\eta}(\mathbf{r})$ is the *average* mesoscopic volume fraction at which $\Omega[\bar{\eta}]$ takes the global minimum, and $H_{fluc}[\bar{\eta}, \psi] = \Omega_{co}[\bar{\eta} + \psi] - \Omega_{co}[\bar{\eta}]$ with $\psi(\mathbf{r})$ denoting the mesoscopic fluctuation (displacement of denser regions with respect to their average positions) [11]. When the fluctuation contribution in Eq.(18) is included as in Ref.[34], then the modulated phases are stable for a smaller region of the phase diagram. In addition, the transition between the disordered and lamellar phases occurs for a larger temperature range [32, 37], in better agreement with simulations [5, 6]. Mesoscopic fluctuations dominate at the high- T part of the phase diagram, therefore for high T this approach is more accurate than mean-field theories. Due to our assumptions ($\phi \ll 1$, $k_b \sigma \ll \pi$), for large values of the OP (i.e. for low T) the microscopic DFT is superior.

Note that Eq.(18) allows for further improvement of the theory by combined DFT and field-theoretic approaches applied to the first and the second term respectively. The first term in (18) can be improved by assuming a more accurate DFT expression for $\Omega_{co}[\bar{\eta}]$. On

the other hand, the dominant fluctuations in the second term in (18) correspond to small values of $\beta H_{fluc}[\bar{\eta}, \psi]$, since the Boltzmann factor $\exp(-a)$ takes negligible values for large a . Thus, the dominant fluctuation contribution comes from small ψ , for which $\Omega_{co}[\bar{\eta} + \psi] - \Omega_{co}[\bar{\eta}]$ can be Taylor expanded, and the field-theoretic methods can be used for evaluation of the second term in (18). Preliminary steps in this direction are described in Ref.[11].

IV. CLASSIFICATION OF THE INTERACTION POTENTIALS

Homogeneous systems can become unstable with respect to the density wave with the wavelength $2\pi/k_b$, when the condition (12) is satisfied. In the case of the density wave of the form $\phi_k \cos(k_b z)$ a region of excess density, π/k_b , is followed by a region of depleted density of the same size. In the case of weak ordering to which this theory is restricted, the density wave does not deviate much from superposition of plane waves in different directions. Effective potentials satisfying (12) can be classified as attraction-dominated ($k_b \approx 0$), repulsion dominated ($k_b \sigma \simeq \pi$) or competing ($0 \ll k_b \sigma \ll \pi$) (Fig.3). The attraction dominated potentials can lead to gas-liquid transition, since the region with excess density, $\pi/k_b \rightarrow \infty$, is macroscopic. The repulsion dominated potentials can lead to periodic ordering of individual particles, since the region with excess density, $\pi/k_b \sim \sigma$ (followed by the region of depleted density of the same size), is comparable with the size of the particles. The competing potentials can lead to excess density in mesoscopic regions, $\sigma \ll \pi/k_b \ll \infty$.

The numerical values of V_n and k_b depend on the shape of the interaction potential and on the approximation for the pair distribution function $g_{co}(r)$, calculated under the constraint of fixed volume fractions in mesoscopic regions, $\eta(\mathbf{r})$. $g_{co}(r)$ is considered as an input from a microscopic theory to our mesoscopic description and should obey $g_{co}(r) \rightarrow 1$ for $r \rightarrow \infty$ and $g_{co}(r) \rightarrow 0$ for $r \rightarrow 0$. Let us compare the results for $g_{co} = 1$ as in simple local DFT theories, and $g_{co}(r) = \theta(r/\sigma - 1)$ (unit step function), for which the contributions to $U[\eta]$ from overlapping hard spheres are not included.

For the double Yukawa potential (Eq.(6)) we have

$$\tilde{V}(k) = 4\pi \left[\frac{K_2}{z_2^2 + k^2} - \frac{K_1}{z_1^2 + k^2} \right] \quad (19)$$

for $g_{co} = 1$, whereas for $g_{co} = \theta(r - 1)$ (we set $\sigma \equiv 1$)

$$\tilde{V}_g(k) = 4\pi \left[\frac{K_2 e^{-z_2}}{z_2^2 + k^2} \left(z_2 \frac{\sin k}{k} + \cos k \right) - \frac{K_1 e^{-z_1}}{z_1^2 + k^2} \left(z_1 \frac{\sin k}{k} + \cos k \right) \right]. \quad (20)$$

Eqs. (20) and (19) are shown for the same parameters in Figs.3 and 4 respectively. Note that except from the pure repulsion, both approximations give similar positions k_b of the global minimum, and similar shape of $\tilde{V}_g(k)$ for $k \approx k_b$, but the value at the minimum is different.

At the crossover between the gas-liquid separation and the periodic ordering the minimum of $\tilde{V}_g(k)$ at $k = 0$ becomes a maximum (Fig.3). Near the crossover the minimum of $\tilde{V}_g(k)$ is shallow (i.e. $\tilde{V}_g''(k_b) \rightarrow 0$). Eq.(13) is valid when the minimum of $\tilde{V}_g(k)$ at $k = k_b$ is deep, therefore it is an oversimplification near the crossover between the gas-liquid separation and the periodic ordering.

In order to easily verify if a given potential leads to microsegregation, we note that at the crossover between gas-liquid separation and periodic ordering the second derivative of $\tilde{V}_g(k)$ at $k = 0$ vanishes. For the double Yukawa potential (Eq.(6)) this happens for $K_2/K_1 = K_{cr}$, where K_{cr} depends on the approximation for g_{co} . The micro-separation or the gas-liquid transition can occur when $K_2/K_1 \gg K_{cr}$ or $K_2/K_1 < K_{cr}$ respectively. When g is neglected as in Eq.(19), we obtain

$$K_{cr} = (z_2/z_1)^4, \quad (21)$$

whereas for $g_{co} = \theta(r - 1)$ from (20) we obtain

$$K_{cr} = \left(\frac{z_2}{z_1} \right)^4 \frac{\left(2 + 2z_1 + z_1^2 + \frac{z_1^3}{3} \right) e^{z_2}}{\left(2 + 2z_2 + z_2^2 + \frac{z_2^3}{3} \right) e^{z_1}}. \quad (22)$$

For $z_1 = 1$ and $z_2 = 0.5$ we have $K_{cr} = 1/16$, or $K_{cr} \approx 0.061$ for $\tilde{V}_g(k)$ given in Eq. (19) or (20), in semiquantitative agreement with $K_{cr} \approx 0.059$ and $K_{cr} \approx 0.053$ in the self-consistent Ornstein-Zernicke approximation (SCOZA) and nonlocal DFT (see Ref.[36]). For increasing z_1 the discrepancy between K_{cr} obtained for the two different forms of g_{co} increases. Nevertheless,

$$K_2/K_1 \gg (z_2/z_1)^4 \quad (23)$$

can serve as a simple condition that must be satisfied by potentials (6) that can lead to microsegregation. Similar criterion was obtained in Refs.[8, 22]. In Ref. [8] the maximum

of the structure factor for $k > 0$ was required for the microsegregation, in analogy to our approach. In Ref. [22] it was assumed that the microsegregation may occur if the energy per particle takes a minimum in a finite cluster.

The structure factor $S(k)$ is more accurate for $g_{co} = \theta(r - 1)$ than for $g_{co} = 1$, because in the first case the contributions to the internal energy from overlapping cores of the particles are not included. The structure factor was obtained in Refs.[11, 12] in an approximation analogous to the random phase approximation (RPA),

$$S(k) = \frac{\tilde{G}(k)}{\rho}, \quad (24)$$

where

$$\tilde{G}(k)^{-1} = \frac{v^2 \delta^2 \beta \Omega_{co}}{\delta \tilde{\eta}(\mathbf{k}) \delta \tilde{\eta}(-\mathbf{k})} = v^2 \left(\beta \tilde{V}_g(k) + \frac{d^2 \beta f_h}{d\eta^2} \right). \quad (25)$$

$S(k)$ takes a maximum at $k = k_b > 0$ for both $g_{co} = \theta(r - 1)$ and $g_{co} = 1$ when ordering on the mesoscopic length scale occurs. Another maximum at $k\sigma \approx 2\pi$, resulting from packing of hard spheres, is present for $g_{co} = \theta(r - 1)$ and absent for $g_{co} = 1$. This second maximum of $\tilde{G}(k)$ results from the minimum of $\tilde{V}_g(k)$ at $k\sigma \approx 2\pi$ (Fig.3).

Further studies are necessary to find the best approximation for g_{co} , and to determine the effect of ordering on the microscopic length scale (described by g_{co}) on the values of V_n . However, our main conclusion that V_2 may be negative when the repulsion is sufficiently strong at large distances ($r \gg \sigma$) remains valid for the pair distribution function $g_{co} > 0$ oscillating around 1 on the microscopic length scale, as in clusters exhibiting internal crystal-like order. The difference between the distribution of the ordered and disordered clusters on the mesoscopic length scale, described by the functional (2), can result from different numerical values of the parameters V_n which are influenced by the form of g_{co} .

V. SUMMARY AND DISCUSSION

We have derived the functional (2) for systems with competing interactions. The same functional (2) was successfully used for amphiphilic systems[25, 26, 32, 33, 37], and in the PFC model of ordering on the atomistic scale [35, 38, 39]. Our result supports on mathematical grounds the hypothesis of universality of microsegregation.

The functional (2) was intensively investigated in the context of block copolymers and microemulsions, and one can take advantage of these earlier results for the SALR systems.

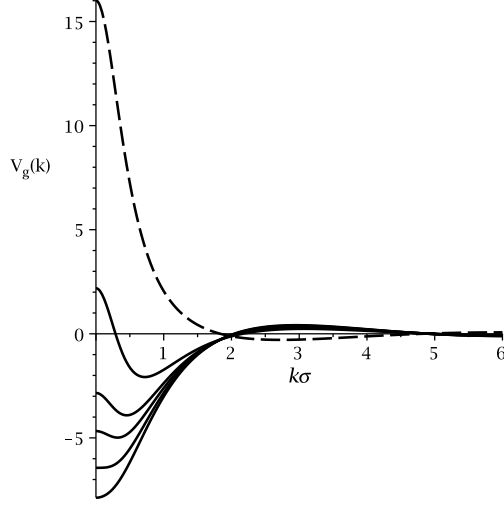


FIG. 3: $\tilde{V}_g(k)$ (Eq.(8)) for the potential (6) and $g = \theta(r/\sigma - 1)$. Dashed line: pure repulsion with $K_1 = 0, K_2/v^2 = 0.35, z_2 = 0.5$. Solid lines: $z_1 = 1, z_2 = 0.5$, and $K_1/v^2 = 1$. From the bottom to the top lines $K_2/v^2 = 0.03, 0.06, 0.1, 0.14, 0.25$.

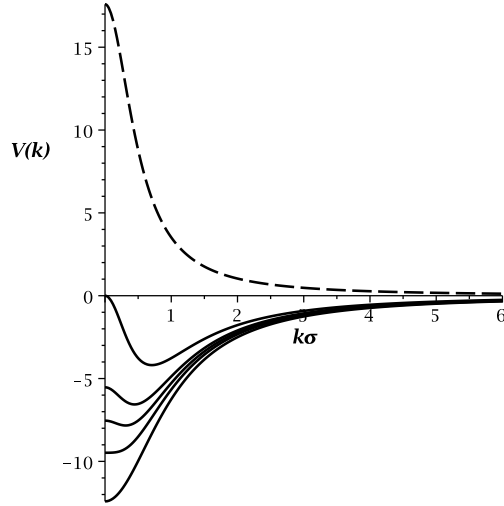


FIG. 4: Fourier transform $\tilde{V}(k)$ (Eq.(19)) of the double Yukawa potential. Dashed line: pure repulsion with $K_1 = 0, K_2/v^2 = 0.35, z_2 = 0.5$. Solid lines: $z_1 = 1, z_2 = 0.5$, and $K_1/v^2 = 1$. From the bottom to the top lines $K_2/v^2 = 0.03, 0.06, 0.1, 0.14, 0.25$.

In particular, based on the very low surface tension between water and microemulsion, we can expect very low surface tension between homogeneous and modulated phases. From the stability or metastability of the bicontinuous phases obtained from the functional (2)[25, 33, 37, 40] we expect thermodynamic stability or metastability of a network of particles (gel)

[12, 37]. In Refs.[5, 23, 41] gel formation was interpreted as arrested microphase segregation. However, stable or very long-lived networks were also found [2, 4, 24, 42]. According to our theory, the stable disordered network should be analogous to a bicontinuous microemulsion or a sponge phase. In addition, an ordered network of particles (gyroid phase) should be thermodynamically stable for a narrow range of thermodynamic variables (Fig.1). In systems with competing interactions such an orderd phase has not been detected experimentally yet. One can expect that aging of gels is influenced by the structure of the thermodynamically stable phase in given thermodynamic conditions. For a narrow range of thermodynamic variables corresponding to stability of the gyroid phase (Fig.1) the percolating structure of the gel should never be destroyed, and may even become more regular. This fact may have practical implications, and verification of our prediction in future experimental and simulation studies or dynamic theories such as PFC [35, 38, 39] is important.

Our considerations concern spherically symmetric (effective) potentials which in Fourier representation have a well-defined minimum for $0 \leq k_b\sigma < \pi$, but otherwise are of arbitrary form. Thus, our conclusions are valid for a wide class of systems. In contrast to previous phenomenological theories, we have obtained microscopic expressions for all the coefficients (Eqs.(5) or (14) and (17)). These expressions allow to predict if for given interactions macro or microsegregation, described by the functional (1) or (2) respectively, should occur. For the particular case of the double Yukawa potential (6) we find a simple criterion (23) for potentials that may lead to microsegregation.

Our functional is very similar to the PFC model, and it is interesting to highlight the similarities and differences between the two theories. The main difference concerns the interpretation of the OP field. In the PFC the OP is the relative local deviation of the density from the space-averaged value, and the PFC is supposed to describe structure formation on the atomistic level. We consider volume fraction of particles averaged over mesoscopic regions, $\eta(\mathbf{r})$, and the OP is the local deviation $\phi(\mathbf{r})$ of this quantity from the space-average value. The $\eta(\mathbf{r})$ describes the volume occupied by the particles within the mesoscopic region around \mathbf{r} , therefore it may correspond to different positions of the particles. Thus, $\eta(\mathbf{r})$ contains less precise information than the microscopic density. As a result of the 'smearing' the particles over mesoscopic regions, the amplitude and the gradient of $\eta(\mathbf{r})$ are both smaller than in the case of the microscopic density. The gradient expansion of $\phi(\mathbf{r})$ in our derivation is better justified than the analogous expansion in derivation of the PFC from

the DFT. Another consequence of the mesoscopic OP is the separation of all fluctuations into microscopic fluctuations for fixed $\eta(\mathbf{r})$ (such as displacements of the particles inside the clusters for fixed distribution of the clusters) and the mesoscopic fluctuations represented by different forms of $\eta(\mathbf{r})$ (such as displacements of the clusters as a whole). Destructive role of mesoscopic fluctuations for periodic ordering on the mesoscopic length scale can be taken into account within field-theoretic methods (see Eq.(18))[11, 34]. On the other hand, in the atomistic-level PFC all fluctuations are considered on the same footing. Derivations of the two theories are based on somewhat different further approximations. We consider separately the internal energy and the entropy. For the latter we assume the hard-sphere form in the local density approximation. In derivation of the PFC from the DFT the free energy is split in the ideal \mathcal{F}_{id} and the excess \mathcal{F}_{ex} parts, and in \mathcal{F}_{ex} terms beyond the quadratic part are neglected. While in our theory the coefficients A_n with $n \geq 3$ are determined by the hard-sphere free energy in the local density approximation, in the PFC they have the ideal gas form. On the other hand, in the PFC the accuracy of the part quadratic in the OP field is limited only by the approximation for the direct correlation function.

On the formal level the direct correlation function in our theory is given by an approximation similar to the RPA (see Eq.(25)), plus the contribution from the mesoscopic fluctuations, obtained from the second term in (18). Let us comment that smaller amplitude of density waves in the PFC than in the DFT [35] could be explained by reinterpretation of the OP along similar lines as in our derivation [11]. On the other hand, dynamics in systems with competing interactions could be described by a theory analogous to the dynamical PFC [35, 38, 39].

Let us finally note that our derivation is based on the assumption that $\tilde{V}_g(k)$ has a single, well defined global minimum for $0 \leq k < \pi$. Physically relevant interaction potentials studied in Refs.[1–3, 5–12, 16, 23, 36] have this property. An exception is the crossover between gas-liquid separation and periodic ordering, where the minimum of $\tilde{V}_g(k)$ is very shallow. However, in general there exist functions with two or more minima with the same or comparable depths for $0 \leq k < \pi$. Such forms of $\tilde{V}_g(k)$ would correspond to simultaneous ordering on different length scales. It is not clear if interactions with such a form of $\tilde{V}_g(k)$ are physically relevant, and if the hierarchical self-assembly may be associated with effective interactions that in Fourier representation have the above mentioned property. Such systems, if exist, cannot be described by the Brazovskii functional (Eq.(2)).

We hope that our predictions can stimulate experimental and simulation studies in this important, but still largely unexplored field. We stress that the periodic order concerns the average density, and due to the presence of fluctuations and large time scales, proper data analysis is required to detect the order on the mesoscopic length scale.

VI. ACKNOWLEDGMENTS

The work of JP was realized within the International PhD Projects Programme of the Foundation for Polish Science, cofinanced from European Regional Development Fund within Innovative Economy Operational Programme "Grants for innovation". AC and WTG acknowledge the financial support by the NCN grant 2012/05/B/ST3/03302

VII. APPENDIX

We derive an approximate expression for the internal energy \mathcal{U} when the local density (or volume fraction) varies on a mesoscopic length scale, i.e. for small gradients of $\rho(\mathbf{r})$. When $\rho(\mathbf{r} + \Delta\mathbf{r})$ is approximated by a truncated Taylor series, Eq.(3) takes the approximate form

$$\mathcal{U} = \frac{1}{2} \int d\mathbf{r} \int d\Delta\mathbf{r} V(\Delta r) g(\Delta r) \rho(\mathbf{r}) \left[\rho(\mathbf{r}) + \Delta r_i \frac{\partial \rho}{\partial r_i} + \frac{1}{2} \Delta r_i \frac{\partial^2 \rho}{\partial r_i \partial r_j} \Delta r_j + \dots \right] \quad (26)$$

where $\mathbf{r} = (r_1, r_2, r_3)$ and summation convention for repeated indexes is used. The above can be written in the form

$$\mathcal{U} = \int d\mathbf{r} \left[V_0 v^2 \rho(\mathbf{r})^2 - \frac{V_2 v^2}{2} \rho(\mathbf{r}) \sum_{i=1}^3 \frac{\partial^2 \rho}{\partial r_i^2} + \dots \right] \quad (27)$$

where $V_0 v^2 = \int d\mathbf{r} V(r) g(r)/2$ and $-V_2 v^2 = \int d\mathbf{r} r_i^2 V(r) g(r)/2$. In derivation of the above we took into account that an integral over R^3 of an odd function, $V(r)g(r)r_i$ and $V(r)g(r)r_i r_j$ with $i \neq j$, vanishes. When the second term in (27) is integrated by parts and the boundary term is neglected, we obtain for \mathcal{U} Eq.(7). Next we take into account that the integration over the angles in spherical variables for any function $f(r)$ of $r = |\mathbf{r}|$ gives

$$\int d\mathbf{r} f(r) = 4\pi \int_0^\infty dr r^2 f(r) \quad (28)$$

and

$$\int d\mathbf{r} f(r) r_i^2 = \frac{4\pi}{3} \int_0^\infty dr r^4 f(r), \quad (29)$$

and for V_0 and V_2 defined above we obtain Eq.(5).

When $V_2 < 0$, the functional in Eq.(7) is unstable, and the Taylor expansion in (26) must be truncated at the fourth order term. The term associated with the third-order derivative vanishes, because the integrand is an odd function. In order to evaluate the fourth-order term, we perform the integration over the angles in spherical variables of the integrands of the form $V(r)g(r)r_i^2r_j^2$ and integrate by parts twice the expressions

$$\int d\mathbf{r}\rho(\mathbf{r})\frac{\partial^4\rho}{\partial r_i^2\partial r_j^2} \quad (30)$$

with $i = j$ as well as $i \neq j$. We neglect the boundary terms, and after some algebra we finally obtain Eqs.(7) and (5).

-
- [1] A. Stradner, H. Sedgwick, F. Cardinaux, W. Poon, S. Egelhaaf, and P. Schurtenberger, *Nature* **432**, 492 (2004).
 - [2] A. I. Campbell, V. J. Anderson, J. S. van Duijneveldt, and P. Bartlett, *Phys. Rev. Lett.* **94**, 208301 (2005).
 - [3] D. E. Masri, T. Vissers, S. Badaire, J. C. P. Stiefelhagen, H. R. Vutukuri, P. Helfferich, T. H. Zhang, W. K. Kegel, A. Imhof, and A. van Blaaderen, *Soft Matter* **8**, 2979 (2012).
 - [4] C. L. Klix, C. P. Royall, and H. Tanaka, *Phys. Rev. Lett.* **104**, 165702 (2010).
 - [5] A. de Candia, E. DelGado, A. Fierro, N. Sator, M. Tarzia, and A. Coniglio, *Phys. Rev. E* **74**, 010403(R) (2006).
 - [6] A. Imperio and L. Reatto, *J. Chem. Phys.* **124**, 164712 (2006).
 - [7] A. J. Archer and N. B. Wilding, *Phys. Rev. E* **76**, 031501 (2007).
 - [8] Tarzia and Coniglio, *Phys. Rev. Lett.* **96**, 075702 (2006).
 - [9] C. Ortix, J. Lorenzana, and C. D. Castro, *Phys. Rev. Lett.* **100**, 246402 (2008).
 - [10] A. J. Archer, *Phys. Rev. E* **78**, 031402 (2008).
 - [11] A. Ciach, *Phys. Rev. E* **78**, 061505 (2008).
 - [12] A. Ciach and W. T. Gózdź, *Condensed Matter Physics* **13**, 23603 (2010).
 - [13] R. Roth, *Mol. Phys.* **109**, 2897 (2011).
 - [14] M. Dijkstra, R. van Roij, and R. Evans, *Phys. Rev. E* **59**, 5744 (1999).

- [15] J. N. Israelachvili, *Intermolecular and Surface Forces (Third Edition)* (Academic Press, Boston, 2011).
- [16] A. Shukla, E. Mylonas, E. D. Cola, S. Finet, P. Timmins, T. Narayanan, and D. I. Sveergun, PNAS **105**, 5075 (2008).
- [17] A. Sanchez-Iglesias, M. Grelczak, T. Altantzis, B. Goris, J. Perez-Juste, S. Bals, G. V. Tondello, S. H. Donaldson, B. F. Chmelka, J. N. Israelachvili, et al., ACS Nano **6**, 11059 (2012).
- [18] S. L. Veatch, O. Soubias, S. L. Keller, and K. Gawrisch, Proc. Nat. Acad. Sci. USA **104**, 17650 (2007).
- [19] C. Hertlein, L. Helden, A. Gambassi, S. Dietrich, and C. Bechinger, Nature **451**, 172 (2008).
- [20] A. Gambassi, A. Maciołek, C. Hertlein, U. Nellen, L. Helden, C. Bechinger, and S. Dietrich, *Phys. Rev. E* **80**, 061143 (2009).
- [21] B. B. Machta, S. L. Veatch, and J. P. Sethna, *Phys. Rev. Lett.* **109**, 138101 (2012).
- [22] S. Mossa, F. Sciortino, P. Tartaglia, and E. Zaccarelli, *Langmuir* **20**, 10756 (2004).
- [23] J. Toledano, F. Sciortino, and E. Zaccarelli, *Soft Matter* **5**, 2390 (2009).
- [24] F. Sciortino, P. Tartaglia, and E. Zaccarelli, *J. Phys. Chem. B* **109**, 21942 (2005).
- [25] G. Gompper and M. Schick, *Self-Assembling Amphiphilic Systems*, vol. 16 of *Phase Transitions and Critical Phenomena* (Academic Press, 1994), 1st ed.
- [26] L. Leibler, *Macromolecules* **13**, 1602 (1980).
- [27] M.W.Matsen and M. Schick, *Curr. Op. Colloid and Interf. Sci.* **1**, 329 (1996).
- [28] M. Seul and D. Andelman, *Science* **267**, 476 (1995).
- [29] N. B. Wilding and P. Sollich, *Europhys Lett.* **101**, 10004 (2013).
- [30] J. L. Barrat and J.-P. Hansen, *Basic Concepts for Simple and Complex Liquids* (Cambridge University Press, 2003).
- [31] D. Andelman, F. Brochard, and J.-F. Joanny, Proc. Nat. Acad. Sci. USA **84**, 4717 (1987).
- [32] G. H. Fredrickson and E. Helfand, *J. Chem. Phys.* **87**, 67 (1987).
- [33] A. Ciach and W. T. Gózdź, *Annu. Rep.Prog. Chem., Sect.C* **97**, 269 (2001), and references therein.
- [34] S. A. Brazovskii, *Sov. Phys. JETP* **41**, 8 (1975).
- [35] H. Emmerich, H. Lwen, R. Wittkowski, T. Gruhn, G. I. Tth, G. Tegze, and L. Grnsy, *Adv. Phys.* **61**, 665 (2012).
- [36] A. J. Archer, D. Pini, R. Evans, and L. Reatto, *J. Chem. Phys.* **126**, 014104 (2007).

- [37] V. E. Podneks and I. W. Hamley, *Pis'ma Zh. Exp. Teor. Fiz.* **64**, 564 (1996).
- [38] A. J. Archer, M. J. Robbins, U. Thiele, and E. Knobloch, *Phys. Rev. E* **46**, 031603 (2012).
- [39] S. van Teeffelen, R. Backofen, A. Voigt, and H. Lwen, *Phys. Rev. E* **79**, 051404 (2009).
- [40] W. T. Gózdź and R. Hołyst, *Phys.Rev.E* **54**, 5012 (1996).
- [41] P. Charbonneau and D. R. Reichman, *Phys. Rev. E* **75**, 050401R (2007).
- [42] E. Zaccarelli, *J. Phys.:Cond. Mat.* **19**, 323101 (2007).